

Preparation of new thermoelectric materials by thin-film technology

M. Hirai¹, T. Mihara² and R. Funahashi²

¹CREST-JST, 4-1-8 Honcho, Kawaguchi, Saitama 332-0012

Fax: 81-72-751-9622, e-mail: manabu-hirai@aist.go.jp

²AIST, 1-8-31 Midorigaoka, Ikeda, Osaka 563-8577

Fax: 81-72-751-9622, e-mail: t-mihara@aist.go.jp, funahashi-r@aist.go.jp

Preparation of superlattices from alternate depositions of $\text{Bi}_2\text{Sr}_2\text{Co}_2\text{O}_9$ and $\text{SrBi}_2\text{Ta}_2\text{O}_9$ has been investigated. Two samples of $[(\text{SrBi}_2\text{Ta}_2\text{O}_9)_1/(\text{Bi}_2\text{Sr}_2\text{Co}_2\text{O}_9)_7]_{10}$ and $[(\text{SrBi}_2\text{Ta}_2\text{O}_9)_1/(\text{Bi}_2\text{Sr}_2\text{Co}_2\text{O}_9)_{10}]_5$ are fabricated in situ using the pulsed laser deposition method. The x-ray diffraction patterns of thin films exhibit the good *c*-axis orientation on the SrTiO_3 (001) substrates. The surface morphology of $[(\text{SrBi}_2\text{Ta}_2\text{O}_9)_1/(\text{Bi}_2\text{Sr}_2\text{Co}_2\text{O}_9)_7]_{10}$ film is observed by atomic force microscopy measurements and is formed stages with altitudes of about 140 nm. Electrical resistivity ρ measurement exhibits hysteresis behavior. The resistivity measured with decreasing temperature is higher than that with increasing temperature, which may be considered due to the decomposition of $\text{Bi}_2\text{Sr}_2\text{Co}_2\text{O}_9$ phase. Seebeck coefficient S of the $[(\text{SrBi}_2\text{Ta}_2\text{O}_9)_1/(\text{Bi}_2\text{Sr}_2\text{Co}_2\text{O}_9)_{10}]_5$ film exhibits $100 \mu\text{VK}^{-1}$ at room temperature. Power factor ($= S^2/\rho$) of the $[(\text{SrBi}_2\text{Ta}_2\text{O}_9)_1/(\text{Bi}_2\text{Sr}_2\text{Co}_2\text{O}_9)_{10}]_5$ film is estimated to be $1.7 \mu\text{Wm}^{-1}\text{K}^{-2}$.

Key words: thermoelectric oxide, thin film, superlattice, power factor

1. INTRODUCTION

Thermoelectric modules using oxide materials have attracted interest in terms of their potential application to clean energy-conversion systems.¹⁻³⁾ Their scale is, however, very large due to the bulk oxide materials which are the main components of modules. In recent years it has been reported that the thermoelectric performance ZT of $\text{Bi}_{2-x}\text{Sb}_x\text{Te}_3$ is significantly enhanced by producing the $\text{Bi}_2\text{Te}_3/\text{SbTe}_3$ superlattice.⁴⁾ ZT is given by

$$ZT = (S^2T/\rho K_T)$$

where S , T , ρ and K_T are the Seebeck coefficient, absolute temperature, electrical resistivity and total thermal conductivity, respectively. The superlattice structure utilizes the acoustic mismatch between the components to reduce lattice thermal conductivity K_L ($K_L = K_T - K_E$, where K_E is the electronic thermal conductivity). At high temperature in air Bi_2Te_3 systems are chemically unstable so that they are unsuitable for application.

The feature of thermoelectric conversion is not effective of the scale or high output density for the injection energy. If this feature is made the best use of, the recovery of a small amount of thermal energy is also possible. However, there are still a lot of problems in a thermoelectric oxide as for the miniaturized modules.

We have developed a good thermoelectric material of $\text{Bi}_2\text{Sr}_2\text{Co}_2\text{O}_9$ (BC222) which is relatively stable at high temperature in air.⁵⁾ BC222 has a layered structure with the CoO_6 octahedron layers which shared edges and the BiO-SrO rock salt block layers stacked alternately as shown in Fig. 1. We expect ZT of such layered compounds to be enhanced by artificially introduced misfit layers to reduce the thermal conductivity.

We have tried to fabricate superlattices of BC222 and

$\text{SrBi}_2\text{Ta}_2\text{O}_9$ (SBT). The crystal structure of SBT consists of Bi_2O_2 layers and double perovskite-type TaO_6 octahedral units, which are similar to Bi-O layers of BC222.⁶⁾ SBT is a good insulator. The *c*-axis length is 25 \AA , which will work not only phonon scattering layers but also electron barrier layers when the superlattices are fabricated.

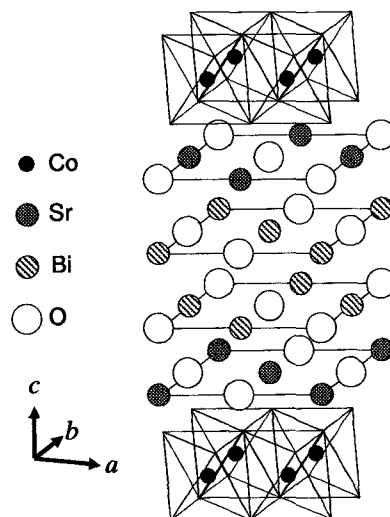


Fig. 1. Schematic illustration of the crystal structure of BC222 ($a = 4.93 \text{ \AA}$, $b = 5.34 \text{ \AA}$, $c = 14.92 \text{ \AA}$). It is composed alternately stacked CoO_6 octahedron layers which shared edges and rock salt block layers along the *c*-axis direction. It has two Bi-O layers in a unit cell.

2. EXPERIMENTAL DETAILS AND RESULTS

All the films were fabricated in situ using PLD (KrF excimer laser COMPex 102 working at 248 nm) with an intensity of 7 Jcm^{-2} and repetition rate of 5 Hz, and were deposited on the SrTiO_3 (001) substrates. The depositing gas was highly pure oxygen (>99.999%). Parallel to each other, the substrate and the target were about 3 cm away. The target was rotated during the ablation process in order to reduce nonuniform erosion. The temperature of heater was from 650°C to 670°C .

X-ray diffraction patterns of the samples were measured using a diffractometer (RINT 2000, Rigaku) with monochromatized $\text{Cu K}\alpha$ radiation. The c -axis length of SBT and BC222 thin films was determined by the (0018) and (0010) diffraction, respectively. Surface morphology and roughness of the films were measured by atomic force microscopy (AFM) in tapping mode (SPI3700, Seiko Instruments Inc.). Electrical resistivity was measured from room temperature to 670°C in air using a conventional four-probe dc method. Seebeck coefficient was calculated from a plot of thermoelectric voltage against temperature difference at room temperature in air using an instrument designed by our laboratory. Two Pt-Pt/Rh (Type-R) thermocouples were attached directly to the films. The heater is attached to the one. Measured relative Seebeck coefficient values were reduced by those of Pt wires to obtain the net Seebeck coefficient S values of the samples.⁷⁾ Power factor PF was calculated from measured ρ and S ($PF = S^2/\rho$).

The starting materials of targets were Bi_2O_3 , SrCO_3 , Ta_2O_5 and Co_3O_4 . The nominal compositions were $\text{Bi}_2\text{Sr}_2\text{Co}_2\text{O}_9$ and $\text{SrBi}_2\text{Ta}_2\text{O}_9$, and the mixtures were heated at 850°C for 30 hours and 1000°C for 24 hours, respectively.

At the first step BC222 and SBT were deposited individually on SrTiO_3 (001) substrate to check their epitaxies. The c -axis oriented thin films were grown on the SrTiO_3 substrate for both materials. At the next step BC222 and SBT were deposited on the same substrate separately. Both BC222/SBT and SBT/BC222 films were grown with the c -axis orientation. Figure 2 shows the x-ray diffraction pattern of SrTiO_3 /SBT/BC222 film.

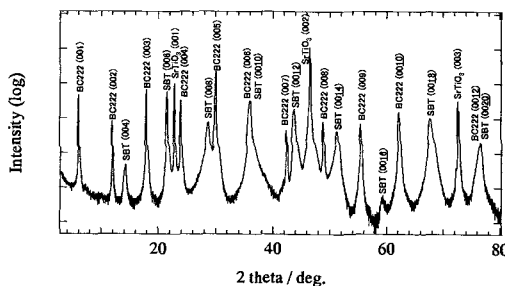


Fig. 2. X-ray diffraction pattern for the c -axis oriented BC222 and SBT thin film on a SrTiO_3 (001) substrate. The c -axis length was 24.90 \AA and 14.91 \AA , respectively.

Deposition rates of SBT and BC222 films were 0.49 \AA/sec and 0.53 \AA/sec , respectively, determined from deposition time and the

thickness of the first films which were measured using a surface profilometer (DEKTAK3, Veeco). Conditions of preparation of superlattices were summarized in Tables I and II.

Table I. Deposition times of samples.

Sample	Deposition time (sec)		Repeat (times)
	SBT	BC222	
A	51	197	10
B	51	281	5

Table II. Summary of the thicknesses calculated from deposited conditions.

sample	Structure	Thickness (\AA)		
		SBT	BC222	Total
A	$(\text{SBT}_1/\text{BC222}_7)_{10}$	25	104	1290
B	$(\text{SBT}_1/\text{BC222}_{10})_5$	25	149	870

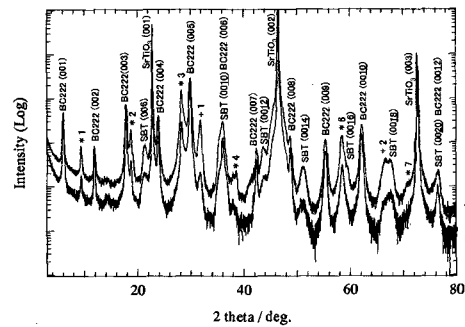


Fig. 3. X-ray diffraction patterns for samples A and B. Diffraction peaks of (00 l) for BC222 and SBT were indicated. The symbols of * and + were indexed by d -values of 9.4 \AA and 2.80 \AA , respectively

Figure 3 shows x-ray diffraction patterns of samples A and B. Diffraction peaks of (00 l) for BC222 and SBT were indexed in the figure. Diffraction peaks were indicated by * and + indexed by d -values of 9.4 \AA and 2.80 \AA , respectively.

Figure 4 shows an AFM image of the sample A. The surface of the film formed stages with altitudes of about 140 nm . Figure 5 shows an AFM image of the SBT thin film. The deposition conditions were the same to the mono layer of samples A or B. Holes and flat stages were seen on the surface of the film, which is called a hole stage image. This image is a process of a flat surface.

In order to measure the electrical resistivity, electrodes were attached to the cross section of the thin film because SBT was a good insulator. Figure 6 shows a picture of sample A. The laser was used in order to scar the thin film and substrate as shown in Fig. 7. Silver paste was run into the scratch in order to cover the side of thin film. Figure 8 shows temperature dependence of electrical resistivity. Seebeck coefficient S , resistivity ρ and power factor PF at room temperature of the samples are summarized in Table III.

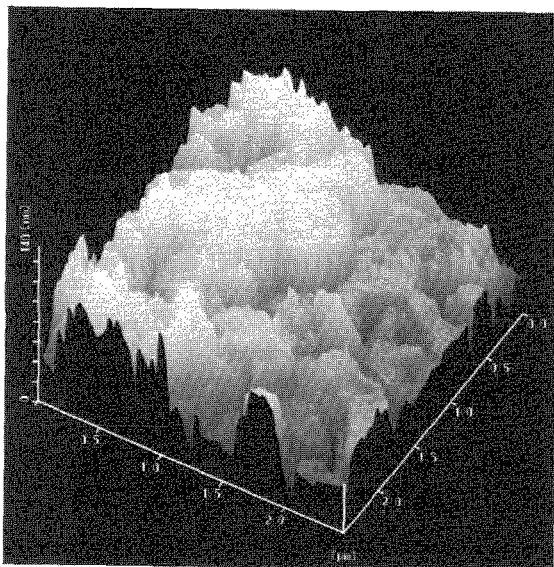


Fig. 4. AFM image of sample A. The surface of the film was formed stages with altitudes of about 140 nm.

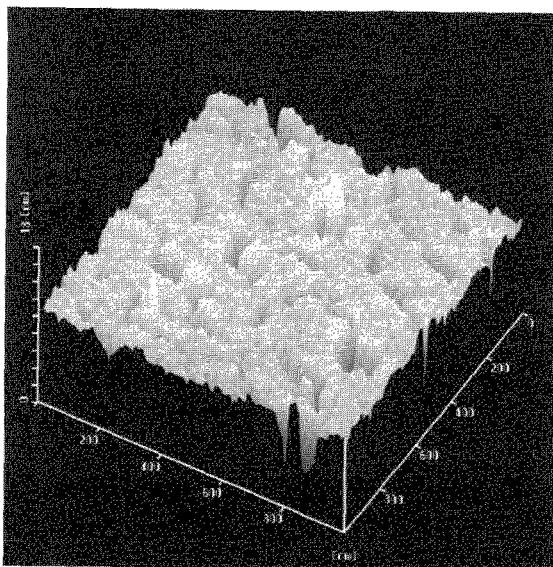


Fig. 5. AFM image of the SBT thin film. The surface morphology was a hole stage image.

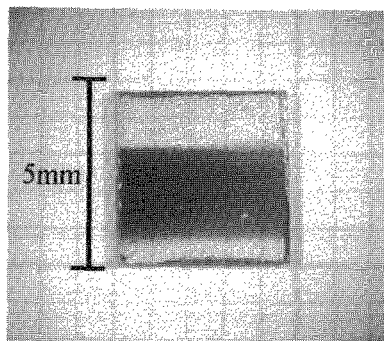


Fig. 6. Picture of sample A.

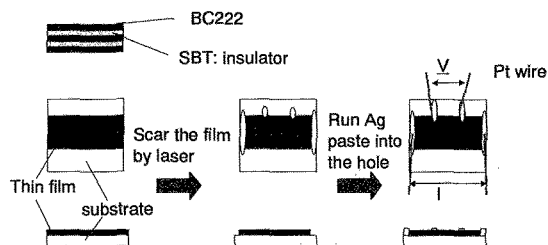


Fig. 7. Schematic illustrations of constructing electrodes.

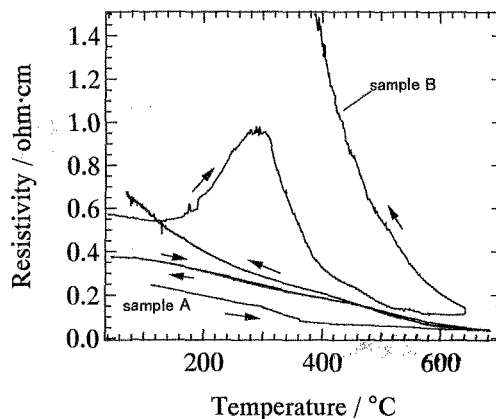


Fig. 8. Temperature dependence of resistivity for samples A and B. Hysteresis behavior was observed.

Table III. Summary of thermoelectric properties of the samples.

Sample	ρ (ohm·cm)	S (μVK^{-1})	PF ($\mu\text{Wm}^{-1}\text{K}^{-2}$)
A	0.3	-	-
B	0.6	100	1.7

3. DISCUSSION

The AFM image of sample A revealed the surface of the thin film is not uniform. The difference of altitude was about 140 nm. The height is higher than 10 times of 104 Å, namely the nominal thickness of the top layer. SBT thin film was, however, almost uniform. This implies that the second layer, namely BC222 thin film, is not uniform. We have to optimize the conditions for BC222.

Least common multiple of 2 kinds of d -values was calculated to be 131.6 Å. This value is somewhat larger than 129 Å (the thickness of (SBT₁/BC222₇)), however, we cannot understand why the x-ray pattern of

sample B is quite similar to sample A except for the intensities of BC222 (00 l) diffraction. If the alternating period is 131.6 Å, the l parameters of all the unknown peaks were indexed 14, 28, 42, 47, 56, 84, 94 and 98, respectively. If it is true, we don't know why there is no other peak between these indexes. Anyway our thin film is not enough for the control of the thickness.

Electrical resistivity of the samples exhibits hysteresis behavior. BC222 phase may decompose in high temperature air. The peak around 300 °C for the sample B is not understood.

The S and PF of Sample B were 100 μVK^{-1} and 1.7 $\mu\text{Wm}^{-1}\text{K}^{-2}$, respectively. The PF is too small even if the resistivity is estimated by subtracting the thickness of the insulating layers.⁸⁾ This also sustains that the conduction layers are not uniform.

4. SUMMARY

In summary, alternating deposition of thin films of BC222 and SBT were tried to prepare on SrTiO₃ substrate by the PLD method. Large altitude of about 140 nm was recognized on the surface of the (SBT₁/BC222₇)₁₀ film. If the problem on this surface is improved, the thin film that we expect will be fabricated. Hysteresis behavior of electrical resistivity was observed, the value with decreasing temperature being higher than that with increasing temperature, and the values of sample A were better than those of sample B. This implies that there is a possibility that the BC222 phase decomposed and the thin BC222 layers are better than thick ones for resistivity and decomposition.

REFERENCES

- [1] R. Funahashi, S. Urata, K. Mizuno, T. Kouuchi and M. Mikami, *Appl. Phys. Lett.*, **85**, 1036-1038 (2004).
- [2] I. Matsubara, R. Funahashi, T. Takeuchi, S. Sodeoka, T. Shimizu and K. Ueno, *Appl. Phys. Lett.*, **78**, 3627 (2001).
- [3] W. Shin, N. Murayama, K. Ikeda and S. Sano, *J. Power Sources*, **103**, 80 (2001).
- [4] R. Venkatasubramanian, E. Siivola, T. Colpitts and B. O'Quinn, *Nature*, **413**, 597-602 (2001).
- [5] R. Funahashi, S. Urata, M. Mikami, K. Mizuno, T. Kouuchi and K. Chong, Proc. 2003 MRS Fall Meeting (Materials Research Society, Boston, 2003), p81
- [6] Y. Shimakawa, Y. Kubo, Y. Nakagawa, T. Kamiyama, H. Asano and F. Izumi, *Appl. Phys. Lett.*, **74**, 1904-1906 (1999).
- [7] J. P. Moore and R. S. Graves, *J. Appl. Phys.*, **44**, 1174-1178 (1973).
- [8] G. Xu, R. Funahashi, M. Shikano, I. Matsubara and Y. Zhou, *J. Appl. Phys.*, **91**, 4344-4347 (2002).

(Received December 11, 2005; Accepted March 31, 2006)